Strong Evidence for Nucleon Resonances near 1900 MeV

A. V. Anisovich,[1,2] V. Burkert,[3] M. Hadžimehmedović,[4] D. G. Ireland,[5] E. Klempt,[1,3] V. A. Nikonov,[1,2] R. Omerović,[4] H. Osmanović,[4] A. V. Sarantsev,[1,2] J. Stahov,[4] A. Švarc,[6] and U. Thoma[1]

[1]*Helmholtz–Institut für Strahlen–und Kernphysik, Universität Bonn, 53115 Bonn, Germany*
[2]*National Research Centre "Kurchatov Institute," Petersburg Nuclear Physics Institute, Gatchina 188300, Russia*
[3]*Thomas Jefferson National Accelerator Facility, Newport News, Virginia 23606, USA*
[4]*University of Tuzla, Faculty of Natural Science and Mathematics, Univerzitetska 4, 75000 Tuzla, Bosnia and Herzegovina*
[5]*SUPA, School of Physics and Astronomy, University of Glasgow, Glasgow G12 8QQ, United Kingdom*
[6]*Rudjer Boskovic Institute, Bijenicka cesta 54, P.O. Box 180, 10002 Zagreb, Croatia*

(Received 23 February 2017; published 11 August 2017)

Data on the reaction $\gamma p \to K^+\Lambda$ from the CLAS experiments are used to derive the leading multipoles, E_{0+}, M_{1-}, E_{1+}, and M_{1+}, from the production threshold to 2180 MeV in 24 slices of the invariant mass. The four multipoles are determined without any constraints. The multipoles are fitted using a multichannel $L+P$ model that allows us to search for singularities and to extract the positions of poles on the complex energy plane in an almost model-independent method. The multipoles are also used as additional constraints in an energy-dependent analysis of a large body of pion and photoinduced reactions within the Bonn-Gatchina partial wave analysis. The study confirms the existence of poles due to nucleon resonances with spin parity $J^P = 1/2^-$, $1/2^+$, and $3/2^+$ in the region at about 1.9 GeV.

DOI: 10.1103/PhysRevLett.119.062004

"Three quarks for Muster Mark" [1]. This sentence inspired Gell-Mann [2] to call quarks the three constituents of nucleons, of protons or neutrons. As a three-body system, the nucleon is expected to exhibit a large number of excitation modes. The most comprehensive predictions of the resonance excitation spectrum stem from quark-model calculations [3–8]; this predicted spectrum is qualitatively confirmed by recent lattice QCD calculations [9], even though the quark masses used lead to a pion mass of 396 MeV. The predicted resonances may decay into a large variety of different decay modes. The most easily accessible was, for a long time, the πN decay of nucleon excitations by studying $\pi^\pm p$ elastic scattering and the $\pi^- p \to \pi^0 n$ charge exchange reaction. A large amount of data was analyzed by the groups at Karlsruhe-Helsinki (KH) [10], Carnegie-Mellon [11] and at GWU [12]. Real and imaginary parts of partial wave amplitudes with defined spin and parity (J^P) were extracted in slices of the πN invariant mass, and resonant contributions were identified. However, only a small fraction of the predicted energy levels has been observed experimentally, and for some of them, the evidence for their existence is only fair or even poor [13,14].

The small number of observed excitations of the nucleon, as compared to quark-model calculations, led to a number of speculations: Are nucleon resonances quark-diquark oscillations with quasistable diquarks [15–19]? Are resonances generated by meson-baryon interactions [20–25], and are quarks and gluons misleading as degrees of freedom to interpret the excitation spectrum? Does the mass degeneracy of high-mass baryon resonances with positive and negative-parity hadron resonances indicate the onset of a new regime in which chiral symmetry is restored [26–28]? At low excitation energy, chiral symmetry is strongly violated as indicated by the large mass gap between the nucleon mass (with spin parity $J^P = 1/2^+$) and its chiral partner $N(1535)$ with $J^P = 1/2^-$. A more conventional interpretation assumes that the missing resonances may have escaped detection due to their small coupling to the πN channel [29]. Some evidence exists, however, that resonances in this mass region can be produced by electromagnetic excitation and decay into $K^+\Lambda$ [14]. Thus, the photoproduction reaction $\gamma p \to K^+\Lambda$ bears the promise of revealing the existence of resonances that are only weakly coupled to πN. Fits to pion and photoproduced reactions have been performed by several groups [BnGa [30], EBAC (KEK-Osaka-Argonne) [31], Gießen [32], JüBo [33], MAID [34], SAID [35], and others], and a number of resonances have been reported [36]. The resonances stem from energy-dependent fits to the data. The resonances and the background contributions in all partial waves need to be determined in a single step. New data on $\gamma p \to K^+\Lambda$ enable a reconstruction of the photoproduction multipoles as functions of energy. The multipoles drive the excitation of one partial wave; hence the fits need to determine only resonances—and the background—contributing to a single partial wave.

The photoproduction of pseudoscalar mesons with an octet baryon in the final state is governed by four complex amplitudes $\mathcal{F}_i, i = 1, \ldots, 4$ [37]. The $\mathcal{F}_i$ are functions of the invariant mass W and of the center-of-mass scattering angle θ. These four amplitudes determine fully the outcome

of any experiment. A determination of the four complex $\mathcal{F}_i$ amplitudes obviously requires the measurement of at least seven different observables as functions of W and θ, and one phase remains undetermined. A more detailed study shows that such a model-independent amplitude analysis requires the measurement of at least eight carefully chosen observables of sufficient statistical accuracy [38,39].

Recently, the CLAS collaboration reported precise data on the process $\gamma p \to K^+\Lambda$. The differential cross section $d\sigma/d\Omega$ and the Λ recoil polarization P were given in [40], the polarization transfer from circular photon polarization to the Λ hyperon C_x and C_z in [41], and the beam asymmetry Σ, the target asymmetry T, and the polarization transfer from linear photon polarization to the Λ hyperon O_x, O_z in [42]. While these represent eight measured observables, data using a polarized target are still required to meet the requirements for fully reconstructing the photoproduction amplitudes at each value of W and θ. Alternatively, the angular dependence can be exploited, and the multipoles can be fitted directly. This reduces the number of observables and the statistical precision of the data that are required to get a fit [43].

In this paper, we determine the multipoles driving the process $\gamma p \to K^+\Lambda$ in 20 MeV wide slices of $K^+\Lambda$ invariant mass. The formalism used to determine multipoles from data is described in [44] where a first attempt was made to determine multipoles in slices of invariant mass. The observables are related to the $\mathcal{F}_i$ amplitudes; here we give one example. The recoil polarization P is given by

$$\begin{aligned} PI &= \sin(\theta)\mathrm{Im}[(2\mathcal{F}_2^* + \mathcal{F}_3^* + \cos(\theta)\mathcal{F}_4^*)\mathcal{F}_1 \\ &\quad + \mathcal{F}_2^*(\cos(\theta)\mathcal{F}_3 + \mathcal{F}_4) + \sin^2(\theta)\mathcal{F}_3^*\mathcal{F}_4], \quad \text{with} \\ I &= \mathrm{Re}[\mathcal{F}_1\mathcal{F}_1^* + \mathcal{F}_2\mathcal{F}_2^* - 2\cos(\theta)\mathcal{F}_2\mathcal{F}_1^* + \frac{\sin^2(\theta)}{2} \\ &\quad \times (\mathcal{F}_3\mathcal{F}_3^* + \mathcal{F}_4\mathcal{F}_4^* + 2\mathcal{F}_4\mathcal{F}_1^* + 2\mathcal{F}_3\mathcal{F}_2^* \\ &\quad + 2\cos(\theta)\mathcal{F}_4\mathcal{F}_3^*)]. \end{aligned} \tag{1}$$

Once the $\mathcal{F}_i$ functions are known, they can be expanded into associated Legendre functions $P_L(\cos\theta)$ and their derivatives $P'_L(\cos\theta)$ with orbital angular momenta L between the K^+ and Λ. We have, e.g.,

$$\mathcal{F}_2(W,\cos\theta) = \sum_{L=1}^{\infty}[(L+1)M_{L+} + LM_{L-}]P'_L(\cos\theta). \tag{2}$$

$E_{L\pm}$ and $M_{L\pm}$ are electric and magnetic multipoles driving final states with defined orbital angular momentum L between meson and baryon and a total spin and parity $J^P = (L \pm 1/2)^{\pm}$. Similar relations hold for the other three $\mathcal{F}_i$ functions [44].

The number of multipoles increases considerably when higher orbital angular momenta are admitted, and extremely precise data are required. Even then, for each slice in energy and angle one phase remains undetermined. Hence one has to suppose that the phase of one multipole amplitude is known that one might take from an energy-dependent fit. Clearly, this introduces some model dependence into the analysis.

Alternatively, the Legendre expansion of $\mathcal{F}_i$ functions (2) can be inserted into the expressions for the polarization observables (1). In principle, this is an infinite series that needs to be determined. However, one can either truncate the power series at a given L, or one can take the high-L multipoles from a model. We use the high-L multipoles from a variety of solutions of the Bonn-Gatchina (BNGA) fits [30].

Figure 1 shows data on $\gamma p \to K^+\Lambda$ for one mass bin and with three fit curves. The data on C_x, C_z, given in wider mass bins, are mapped onto 20 MeV bins and are used in addition. The red (dotted) curves in Fig. 1 show the result of a single-energy fit to the data. With the given accuracy of the data, we found that only a small number of multipoles, E_{0+}, M_{1-}, E_{1+}, M_{1+}, can be determined without imposing additional constraints (like a penalty function that forces the fit not to deviate too much from a predefined solution). The fit determines the real and imaginary parts of these four photoproduction multipoles for one single mass bin. These four multipoles varied freely in the fit, with no constraint. They excite resonances with the quantum numbers $J^P = 1/2^+$, $1/2^-$, and $3/2^+$. Three further multipoles, E_{2-}, M_{2-}, E_{2+} driving excitations to $J^P = 3/2^-$ and $5/2^-$, were constrained to the energy-dependent BNGA fit by a penalty function that forces the fit not to deviate too much from the predefined solution. The higher mutipoles (up to $L < 9$) were fixed to the energy-dependent BNGA fit. These multipoles also provide the overall phase.

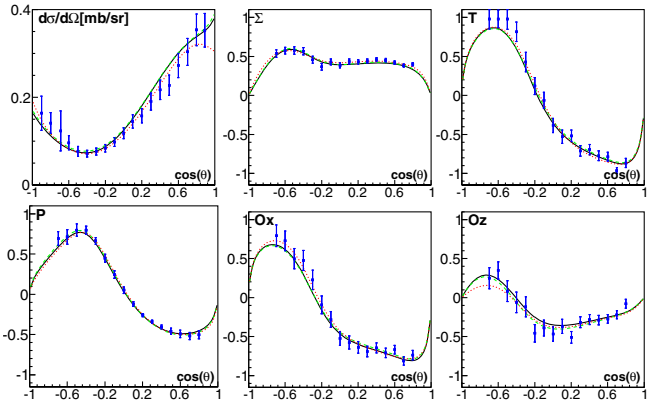

FIG. 1. Example of a fit to the data for the mass range from 1950 to 1970 MeV. $d\sigma/d\Omega$: [40], P [40], Σ, T, O_x, O_z [42]. The (red) dotted curve corresponds to the fit used to determine the multipoles of Fig. 2, the (black) solid curves to fits using $L + P$ for low-L partial wave and BNGA for high-L, and the (green) dashed curves to the BNGA fit.

TABLE I. Properties of nucleon resonances from the Particle Data Group (PDG) estimates [14], the BNGA PWA fit, and $L+P$ fits. Masses and widths are given in MeV, the normalized inelastic pole residues $2g^a(\pi N \to K\Lambda)/\Gamma_a$ are numbers.

	$J^P = 1/2^-$			$J^P = 1/2^+$			$J^P = 3/2^+$		
	PDG	BNGA	M$CL+P$	PDG	BNGA	M$CL+P$	PDG	BNGA	$L+P$
M_1	1640–1670	1658 ± 10	1660 ± 5	1670–1770	1690 ± 15	1697 ± 23	⋯	⋯	⋯
Γ_1	100–170	102 ± 8	59 ± 16	90–380	155 ± 25	84 ± 34	⋯	⋯	⋯
$\lvert\mathrm{Re}s_1(\pi N \to K\Lambda)\rvert$		0.26 ± 0.10	0.10 ± 0.10	⋯	0.16 ± 0.05	$0.12^{+0.24}_{-0.12}$	⋯	⋯	⋯
Θ_1	⋯	$(110 \pm 20)^0$	$(95 \pm 33)^0$	⋯	$-(160 \pm 25)^0$	$-(119 \pm 83)^0$	⋯	⋯	⋯
M_2	⋯	1895 ± 15	1906 ± 17	⋯	1860 ± 40	1875 ± 11	1900–1940	1945 ± 35	1912 ± 30
Γ_2	⋯	132 ± 30	100 ± 10	⋯	230 ± 50	33 ± 9	130–300	135^{+70}_{-30}	166 ± 30
$\lvert\mathrm{Re}s_2(\pi N \to K\Lambda)\rvert$	⋯	0.09 ± 0.03	0.06 ± 0.02	⋯	0.05 ± 0.02	0.30 ± 0.10	⋯	0.03 ± 0.02	⋯
Θ_2	⋯	$(8 \pm 30)^0$	$(87 \pm 27)^0$	⋯	$(27 \pm 30)^0$	$(82 \pm 9)^0$	⋯	$(90 \pm 40)^0$	⋯

Figure 1 shows two more fits: the solid curves represent the $L+P$ fit (described below), the dashed curves the energy-dependent BNGA fit. The results of the BNGA fits are shown in Table I. In the fits, different BNGA starting fits were used that resulted from different fit hypotheses. In particular, high-mass resonances with spin parities $J^P = 1/2^\pm, \ldots, 7/2^\pm$ were added to the fit hypothesis. The spread of the results was used to derive the errors given in Table I.

Figure 2 shows the multipoles as functions of the mass. The statistical errors are determined by a scan of the χ^2 dependence of the single-energy fit on one of the multipoles while the other multipoles vary freely. The χ^2 of this fit includes the statistical and systematic errors of the data. The systematic errors for the real part are given at the top of the subfigures, those for the imaginary part on the bottom. The systematic errors are determined by using different energy-dependent BNGA fits, used to constrain the multipoles E_{2-}, M_{2-}, E_{2+} and to determine the higher partial waves. The different energy-dependent BNGA fits include, one by one, additional high-mass resonances (with weak evidence for their existence) in each partial wave. At small masses, there are visible differences between the $L+P$ fit and the BNGA fit. These can be traced to the lack of polarization data at low energies in the backward region.

First, we notice that all fitted multipoles show strong variations as functions of the mass. It therefore seems obvious that there are strong resonant contributions. Indeed, a first simple fit with Breit-Wigner amplitudes plus a polynomial background shows that resonant contributions are necessary for all four multipoles to achieve a good fit.

In this paper, we use a Laurent (more precisely Mittag-Leffler [45]) method [46–52], called the $L+P$ method, to separate the singularities and the regular parts. The background is represented by analytic functions with well-defined cuts. The method was described by Ciulli and Fischer in [53] and extensively used in the KH description of πN scattering [10] (details are described by Pietarinen in [54,55]). The method is (almost) model independent. No dynamical assumptions are made except that the scattering amplitude is an analytic function in the complex energy plane with singularities due to poles and thresholds.

The transition amplitude of the $L+P$ model is parametrized as

$$T^a(W) = \sum_{j=1}^{N_{\mathrm{pole}}} \frac{g_j^a}{W_j - W} + \sum_{i=1}^{3} \sum_{k_i=0}^{K^a} c_{k_i}^a \left(\frac{\alpha_i^a - \sqrt{x_i^a - W}}{\alpha_i^a + \sqrt{x_i^a - W}} \right)^{k_i}, \tag{3}$$

where a is a channel index, W_j are pole positions in the complex W (energy) plane, and g_j^a are residues for $\pi N \to K\Lambda$ transitions. The x_i^a define the branch points, $c_{k_i}^a$, and α_i^a

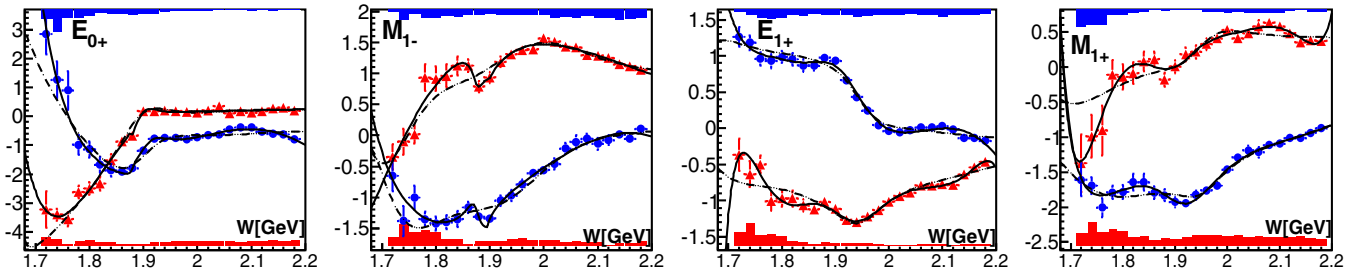

FIG. 2. Real (red triangles) and imaginary (blue dots) part of the E_{0+}, M_{1-}, E_{1+}, and M_{1+} multipoles for the reaction $\gamma p \to K^+\Lambda$. The systematic errors are given at the top (real part) and bottom (imaginary part) of the subfigures. E_{0+} excites the partial wave $J^P = 1/2^-$, M_{1-}: $J^P = 1/2^+$, E_{1+} and M_{1+}, $J^P = 3/2^+$. The solid curve shows the $L+P$ fit, the dashed curve the energy-dependent BNGA fit.

are real coefficients. $K^a, L^a, M^a, \ldots$ are the number of Pietarinen coefficients in channel a. The first part represents the poles and the second term three branch points. The first branch point is chosen to describe all subthreshold and left-hand cut processes, the second one is fixed to the dominant channel opening, and the third one represents background contributions of all channel openings in the physical range.

To enable the fitting we define a reduced discrepancy function D_{dp} as

$$D_{dp} = \sum_{a}^{\text{all}} D^a_{dp},$$

$$D^a_{dp} = \frac{1}{2N^a_W - N^a_{\text{par}}} \times \sum_{i=1}^{N^a_W} \left[\left(\frac{\text{Re}T^a(W^{(i)}) - \text{Re}T^{a,\text{exp}}(W^{(i)})}{\text{Err}^{\text{Re}}_{i,a}} \right)^2 + \left(\frac{\text{Im}T^a(W^{(i)}) - \text{Im}T^{a,\text{exp}}(W^{(i)})}{\text{Err}^{\text{Im}}_{i,a}} \right)^2 \right] + \mathcal{P}^a,$$

$$\text{where } \mathcal{P}^a = \lambda^a_{k_1} \sum_{k_1=1}^{K^a} (c^a_{k_1})^2 {k_1}^3 + \lambda^a_{k_2} \sum_{k_2=1}^{L^a} (c^a_{k_2})^2 {k_2}^3 + \lambda^a_{k_3} \sum_{m=1}^{M^a} (c^a_{k_3})^2 {k_3}^3$$

is the Pietarinen penalty function that ensures fast and optimal convergence.

N^a_W is the number of energies in channel a, N^a_{par} is the number of fit parameters in channel a, $\lambda^a_c, \lambda^a_d, \lambda^a_e$ are Pietarinen weighting factors, $\text{Err}^{\text{Re,Im}}_{i,a}$.... are errors of the real and imaginary part, and $c^a_{k_1}, c^a_{k_2}, c^a_{k_3}$ real coupling constants.

Figure 2 shows the $L+P$ fit. This fit follows the data much more precisely than the BNGA fit. The reason is, of course, that BNGA fits the real data while $L+P$ represents a fit to the data in Fig. 2.

In addition to the data on $\gamma p \to K^+\Lambda$ discussed here (channel $a=1$), we included in the fits the amplitudes T_{J^P} for $\pi^- p \to K^0\Lambda$ (channel $a=2$) [56] since they provide the information on the $\pi N \to K\Lambda$ transition residues and allowed for a better determination of the low-mass poles at the $K\Lambda$ threshold. The photoproduction data alone determine well the properties of the resonance at about 1900 MeV but not the poles at the $K\Lambda$ threshold. The $N(1720)3/2^+$ resonance cannot be determined reliably from the $K\Lambda$ final states.

E_{0+} and $T_{1/2^-}$: First, the branch points were fixed to the πN, $K^+\Lambda$, and the $\eta' p$ thresholds. A fit with one pole failed to reproduce both channels, and a second pole was added. The fit gave a reasonable description of the data and was slightly improved when the second and third branch points were released to adjust to close-by values. The results of the fit are given in Table I. The agreement between the BNGA and the $L+P$ fit is excellent. We consider the existence of both resonances as certain and its properties as reasonably well defined.

M_{1-} and $T_{1/2^+}$: The procedure was repeated for the $J^P = 1/2^+$ partial wave. Again, the fits require two resonances, in particular, the new $N(1880)1/2^+$ state, but it turns out to be rather narrow. The second branch point was fixed at the $K^+\Lambda$ threshold, the third one moved to $x_3 = 1.898$ GeV. The result of the $L+P$ and the BNGA fits are given in Table I. The existence of both resonances is mandatory in both fits. However, there is a discrepancy in the width. We changed the binning by shifting the bins by 10 MeV and by choosing 25 MeV bins; the narrow structure in the $L+P$ fit remained. The narrow width is however incompatible with the BNGA fit: when a $N(1880)1/2^+$ width of 42 MeV was imposed, the overall χ^2 deteriorated by 1000 units, and the fit visibly missed describing the data properly.

When a $N(1880)1/2^+$ width of 150 MeV was imposed in the $L+P$ fit, it deteriorated from $\chi^2 = 16.7$ for 76 data points and 43 parameters to $\chi^2 = 24.9$ for 40 parameters. Compared to the actual data, the difference of the main $L+P$ fit (with 33 MeV width) and the test fit (with 150 MeV width) is marginal. For the 674 data points, the improvement in χ^2 is 4.5 only. This gain does not justify claiming a narrow structure in the M_{1-} multipole. It seems that, in the energy-independent analysis, small systematic deviations from the "true" values create a narrow structure that can be interpreted as a narrow resonance. The existence of $N(1880)1/2^+$ is certain but the $N(1880)1/2^+$ width is not well defined, likely due to a statistical fluctuation (or a systematic deviation) in one of the data sets.

E_{1+} and M_{1+}: In this case, only single-channel analyses were performed as the data from the $\pi^- p \to K^0\Lambda$ process were of insufficient quality. In particular, the properties of $N(1720)3/2^+$ could not be deduced from the fits. The E_{1+}, M_{1+} multipoles were fitted simultaneously with identical pole positions, the same branch points but with free Pietarinen coefficients. The second branch point was fixed to the $K\Lambda$ threshold, and the third branch point converged to $x_3 = 2.46$ GeV. The results of the fit are reproduced in Table I. We consider the existence of the $N(1900)3/2^+$ resonance as certain and its properties as reasonably well defined.

The use of two independent approaches, one energy independent and one energy dependent allowed us to draw definitive conclusions about the existence of several excited

nucleon states. So far, the evidence for two of these resonances was estimated by the PDG to be fair only. These two resonances, $N(1880)1/2^+$ and $N(1895)1/2^-$, are presently not included in the PDG baryon summary table and are mostly not taken into account when models of baryons are compared to data. Establishing the existence of nucleon resonances in this mass range is therefore of great importance.

Summarizing, we have determined low-L multipoles for the reaction $\gamma p \to K^+\Lambda$. The multipoles were fitted using the Laurent-Pietarinen method, which has minimal model dependence. The fits firmly establish the existence of three resonances and determine their properties. This opens up a promising new avenue of the field of baryon spectroscopy with electromagnetic probes.

This work is supported by the Deutsche Forschungsgemeinschaft (Grant No. SFB/TR110, SFB1044), U.S. Department of Energy, U.S. National Science Foundation, U.K. Science and Technology Facilities Council (Grant No. ST/L005719/1), and the Russian Science Foundation (Grant No. RSF 16-12-10267).

[1] J. Joyce, *Finnegan's Wake* (Faber & Faber, London, 1939).
[2] M. Gell-Mann, *The Quark and the Jaguar* (W. H. Freeman and Company, New York, 1994).
[3] S. Capstick and N. Isgur, Phys. Rev. D **34**, 2809 (1986).
[4] L. Y. Glozman, W. Plessas, K. Varga, and R. F. Wagenbrunn, Phys. Rev. D **58**, 094030 (1998).
[5] U. Löring, B. C. Metsch, and H. R. Petry, Eur. Phys. J. A **10**, 395 (2001).
[6] M. Ronniger and B. C. Metsch, Eur. Phys. J. A **47**, 162 (2011).
[7] E. Santopinto and J. Ferretti, Phys. Rev. C **92**, 025202 (2015).
[8] M. M. Giannini and E. Santopinto, Chin. J. Phys. **53**, 020301 (2015).
[9] R. G. Edwards, J. J. Dudek, D. G. Richards, and S. J. Wallace, Phys. Rev. D **84**, 074508 (2011).
[10] G. Höhler and H. Schopper, *Numerical Data and Functional Relationships in Science and Technology. Group I: Nuclear and Particle Physics. Vol. 9, Elastic and Charge Exchange Scattering of Elementary Particles. B, Pion Nucleon Scattering, Pt. 2, Methods and R* (Springer, Berlin, Germany, 1983), p. 601.
[11] R. E. Cutkosky, C. P. Forsyth, J. B. Babcock, R. L. Kelly, and R. E. Hendrick, in *4th International Conference on Baryon Resonances, Toronto, Canada, 1980* (Toronto University Press, Toronto, 1980).
[12] R. A. Arndt, W. J. Briscoe, I. I. Strakovsky, and R. L. Work-man, Phys. Rev. C **74**, 045205 (2006).
[13] The Particle Data Group classifies baryon resonances with a star rating: * (poor), ** (fair), *** (very likely), and **** (certain).
[14] C. Patrignani *et al.* (Particle Data Group Collaboration), Chin. Phys. C **40**, 100001 (2016).
[15] M. Anselmino, E. Predazzi, S. Ekelin, S. Fredriksson, and D. B. Lichtenberg, Rev. Mod. Phys. **65**, 1199 (1993).
[16] M. Kirchbach, M. Moshinsky, and Y. F. Smirnov, Phys. Rev. D **64**, 114005 (2001).
[17] R. L. Jaffe and F. Wilczek, Phys. Rev. Lett. **91**, 232003 (2003).
[18] R. L. Jaffe, Phys. Rep. **409**, 1 (2005).
[19] E. Santopinto, Phys. Rev. C **72**, 022201 (2005).
[20] R. H. Dalitz, Phys. Rev. Lett. **6**, 239 (1961).
[21] S. Schneider, S. Krewald, and U.-G. Meissner, Eur. Phys. J. A **28**, 107 (2006).
[22] N. Kaiser, P. B. Siegel, and W. Weise, Phys. Lett. B **362**, 23 (1995).
[23] M. F. M. Lutz and E. E. Kolomeitsev, Nucl. Phys. **A755**, 29 (2005).
[24] B. S. Zou, Eur. Phys. J. A **35**, 325 (2008).
[25] M. Mai, P. C. Bruns, and Ulf-G. Meißner, Phys. Rev. D **86**, 094033 (2012).
[26] L. Y. Glozman, Phys. Lett. B **475**, 329 (2000).
[27] L. Y. Glozman, Phys. Lett. B **587**, 69 (2004).
[28] L. Y. Glozman, Phys. Rep. **444**, 1 (2007).
[29] R. Koniuk and N. Isgur, Phys. Rev. Lett. **44**, 845 (1980).
[30] A. V. Anisovich, V. Burkert, E. Klempt, V. A. Nikonov, E. Pasyuk, A. V. Sarantsev, S. Strauch, and U. Thoma, [Phys. Lett. B (to be published)].
[31] H. Kamano, S. X. Nakamura, T.-S. H. Lee, and T. Sato, Phys. Rev. C **94**, 015201 (2016).
[32] V. Shklyar, H. Lenske, and U. Mosel, Phys. Rev. C **87**, 015201 (2013).
[33] D. Rönchen, M. Döring, H. Haberzettl, J. Haidenbauer, U.-G. Meißner, and K. Nakayama, Eur. Phys. J. A **51**, 70 (2015).
[34] V. L. Kashevarov, L. Tiator, and M. Ostrick, Bled Workshops Phys. **16**, 9 (2015).
[35] R. L. Workman, R. A. Arndt, W. J. Briscoe, M. W. Paris, and I. I. Strakovsky, Phys. Rev. C **86**, 035202 (2012).
[36] A. V. Anisovich, R. Beck, E. Klempt, V. A. Nikonov, A. V. Sarantsev, and U. Thoma, Eur. Phys. J. A **48**, 15 (2012).
[37] G. F. Chew, M. L. Goldberger, F. E. Low, and Y. Nambu, Phys. Rev. **106**, 1345 (1957).
[38] See A. M. Sandorfi, S. Hoblit, H. Kamano, and T.-S. H. Lee, J. Phys. G **38**, 053001 (2011), and references therein.
[39] D. G. Ireland, Phys. Rev. C **82**, 025204 (2010).
[40] M. E. McCracken *et al.* (CLAS Collaboration), Phys. Rev. C **81**, 025201 (2010).
[41] R. K. Bradford *et al.* (CLAS Collaboration), Phys. Rev. C **75**, 035205 (2007).
[42] C. A. Paterson *et al.* (CLAS Collaboration), Phys. Rev. C **93**, 065201 (2016).
[43] Y. Wunderlich, R. Beck, and L. Tiator, Phys. Rev. C **89**, 055203 (2014).
[44] A. V. Anisovich, R. Beck, V. Burkert, E. Klempt, M. E. McCracken, V. A. Nikonov, A. V. Sarantsev, R. A. Schumacher, and U. Thoma, Eur. Phys. J. A **50**, 129 (2014).
[45] Michiel Hazewinkel, *Encyclopaedia of Mathematics* (Springer, New York, 1990), Vol. 6, p. 251.
[46] A. Švarc, M. Hadžimehmedović, H. Osmanović, and J. Stahov, arXiv:1212.1295.
[47] A. Švarc, M. Hadžimehmedović, H. Osmanovićs, J. Stahov, L. Tiator, and R. L. Workman, Phys. Rev. C **88**, 035206 (2013).

[48] A. Švarc, M. Hadžimehmedović, R. Omerović, H. Osmanović, and J. Stahov, Phys. Rev. C **89**, 045205 (2014).
[49] A. Švarc, M. Hadžimehmedović, H. Osmanović, J. Stahov, L. Tiator, and R. L. Workman, Phys. Rev. C **89**, 065208 (2014).
[50] A. Švarc, M. Hadžimehmedović, H. Osmanović, J. Stahov, and R. L. Workman, Phys. Rev. C **91**, 015207 (2015).
[51] L. Tiator, M. Döring, R. L. Workman, M. Hadžimehmedović, H. Osmanovć, R. Omerovć, J. Stahov, and A. Švarc, Phys. Rev. C **94**, 065204 (2016).
[52] A. Švarc, M. Hadžimehmedović, H. Osmanović, J. Stahov, L. Tiator, and R. L. Workman, Phys. Lett. B **755**, 452 (2016).
[53] I. Ciulli, S. Ciulli, and J. Fisher, Nuovo Cimento **23**, 1129 (1962).
[54] E. Pietarinen, Nuovo Cimento Soc. Ital. Fis. **12A**, 522 (1972).
[55] E. Pietarinen, Nucl. Phys. **B107**, 21 (1976).
[56] A. V. Anisovich, R. Beck, E. Klempt, V. A. Nikonov, A. V. Sarantsev, U. Thoma, and Y. Wunderlich, Eur. Phys. J. A **49**, 121 (2013).